ENGINEERING MATHEMATICS
AND COMPUTING LAB

UNIVERSITÄT
HEIDELBERG
ZUKUNFT
SEIT 1386

An analytically solvable benchmark problem for fluid-structure interaction with uncertain parameters

Jonas Kratzke, Vincent Heuveline

Preprint No. 2016-02

Preprint Series of the Engineering Mathematics and Computing Lab (EMCL)

http://emcl.iwr.uni-heidelberg.de

Preprint Series of the Engineering Mathematics and Computing Lab (EMCL)
ISSN 2191–0693
Preprint No. 2016-02

Affiliation of the Authors

Jonas Kratzke[a,1], Vincent Heuveline[a]

[a] *Engineering Mathematics and Computing Lab (EMCL), Interdisciplinary Center for Scientific Computing (IWR), Heidelberg University, Germany*
[1] *Corresponding Author: Jonas Kratzke, jonas.kratzke@iwr.uni-heidelberg.de*

Impressum

Heidelberg University
Interdisciplinary Center for Scientific Computing (IWR)
Engineering Mathematics and Computing Lab (EMCL)

Im Neuenheimer Feld 205,
69120 Heidelberg
Germany

An analytically solvable benchmark problem for fluid-structure interaction with uncertain parameters

Jonas Kratzke, Vincent Heuveline

December 21, 2016

In simulating fluid-structure interaction, e.g. for the biomechanical dynamics of aortic blood flow, a profound benchmarking of the numerical solver is a basic prerequisite. We consider a test scenario for a fluid-structure interaction solver including uncertain model parameters that has an analytical solution. The solver is developed to simulate the flow and movement of the human aorta. In simulating the biomechanical dynamics of aortic blood flow, there are usually high uncertainties with respect to the model itself and with respect to the input parameters such as the stiffness of the vessel wall. If numerical simulation is considered to provide assistance in a clinical context, these uncertainties also have to be reflected in the simulation results for reliability.

To verify a solver for fluid-structure interaction with uncertain parameters, we introduce a benchmark problem for which we derive an analytical solution. The benchmark is based on the Taylor-Couette flow system with an additional solid domain surrounding the fluid domain. Whereas the analytical solution is stated in polar coordinates, the problem is non-trivial for solvers based on the Cartesian coordinate system. The stochastic space is discretised by means of a generalised Polynomial Chaos expansion. By Galerkin projection on the stochastic basis, we obtain an intrusive Uncertainty Quantification method. The benchmarking results for the implemented solver are in well accordance with the theoretically expected convergence properties.

1 Introduction

Several test scenarios have been published for the verification and benchmarking of fluid-structure interaction (FSI) simulations, e.g. the flow around a cylinder with an elastic bar by Turek et al. [13] or the benchmarking examples by Bathe et al. [2]. However, to the knowledge of the authors, an FSI benchmark with an analytical solution has not been stated yet, especially for the case of incorporating uncertain parameters. An area, in which the verification of applicable FSI simulations is a basic prerequisite, is given by the biomechanics of blood flow in elastic vessels. Blood flow is modelled by the equations of fluid dynamics. Elasto-mechanical models can describe the movement of the vessel wall. For the interaction of the two phases, suitable coupling conditions at the interface have to be stated [5].

Numerical simulation, such as FSI simulations, can provide crucial information in medical applications. A recent review by Chung and Cebral [3] on the role of numerical simulation in the treatment planning of aneurysms, for example, emphasised the potential of taking simulation results for clinical risk assessment into account. Hereby, medical imaging of blood vessels can be enhanced with additional parameters obtained by blood flow simulations [8]. One of these parameters is given by the wall shear stress which correlates with endothelial cell remodelling by elongation and realignment. Its evaluation can give further indications on the rupture risk of the vessel wall.

The outcome of a numerical simulation is subject to uncertainties on several levels. For reliable information based on simulations, they have to be carefully considered and questioned. The main levels of uncertainties include the modelling of the relevant physiological dynamics, the calibration by medical imaging measurements and data as well as the numerical error with respect to the discretisation and computation. Methods of Uncertainty Quantification can give necessary tools for quantifying the reliability of simulation results [9].

This work presents the benchmarking of a finite element simulation for solving FSI problems with uncertain parameters by means of a test case with an analytical solution.

2 Fluid-structure interaction with uncertain parameters

In general, the biomechanical behaviour of blood flow and vessel wall elasticity is highly complex and patient-specific. Being a solution of blood plasma and cells, blood is a Non-Newtonian fluid. Only in large vessels, it approximately behaves Newtonian [10]. Blood vessel walls consist of two or three layers of different anisotropic nonlinear soft tissue materials [7]. For the ease of benchmarking an implementation of a fluid-structure interaction simulation, we focus on the incompressible Navier-Stokes equations for the flow field (1), (2) and the linear elasticity equations for the solid material (3). We model the boundary velocity and the stiffness of the solid material as uncertain parameters. The latter addresses the circumstance, that with current medical techniques, the stiffness of a material can only be assessed highly invasive if at all.

The considered stochastic FSI equations are given by

$$(v \cdot \nabla)v + \frac{1}{\rho}\nabla p - \nu\nabla \cdot (\nabla v + \nabla v^T) = 0, \quad \text{in } \mathcal{D}_f \times \Omega, \tag{1}$$

$$\nabla \cdot v = 0, \quad \text{in } \mathcal{D}_f \times \Omega, \tag{2}$$

$$-\nabla \cdot \big(\lambda(\nabla \cdot u)I + \mu(\nabla u + \nabla u^T))\big) = 0, \quad \text{in } \mathcal{D}_s \times \Omega, \tag{3}$$

$$\big(\rho\nu(\nabla v + \nabla v^T) - pI\big)\, n_f + \big(\lambda(\nabla \cdot u)I + \mu(\nabla u + \nabla u^T)\big)\, n_s = 0, \quad \text{on } \mathcal{B}_i \times \Omega. \tag{4}$$

The equations (1) - (4) describe a stationary state of a velocity field v and pressure distribution p in the fluid domain $\mathcal{D}_f$ and a displacement field u on the solid domain $\mathcal{D}_s$. These variables also have a probability distribution over the stochastic space Ω. Equation (4) describes the balance of forces on the fluid-solid interface $\mathcal{B}_i$. The material parameters are given by the density ρ, the kinematic viscosity ν, and the Lamé parameters λ and μ. The latter depend on the Poisson's ratio γ and the Young's modulus Y via the relations

$$\lambda = \frac{Y\gamma}{(1+\gamma)(1-2\gamma)}, \tag{5}$$

$$\mu = \frac{Y}{2(1+\gamma)}. \tag{6}$$

As a measure of stiffness, we model the Young's modulus as stochastically distributed. As the stiffness is hard to assess, we assume a uniform distribution (7) as a so called "ignorance model". Hereby, we do not assume any preferred values of the probability of Y. To close the system of partial differential equations (1) - (4) appropriate Dirichlet and Neumann boundary conditions have to be defined on the outer fluid boundary $\mathcal{B}_f$ and the outer solid boundary $\mathcal{B}_s$. We parametrise the fluid flow Dirichlet boundary conditions with a uniformly distributed parameter V as denoted in (8). The two stochastic parameters of the Young's modulus and the boundary velocity are assumed to be stochastical independent.

$$Y(\omega) := Y_0 + \omega Y_1, \qquad \omega \sim U(-1,1), \tag{7}$$

$$V(\omega) := V_0 + \omega V_1, \qquad \omega \sim U(-1,1). \tag{8}$$

3 A benchmarking problem with an analytical solution

Most benchmarks for FSI simulations rely on the comparison against a highly resolved computation as a reference solution or the comparison of several numerical approaches as it has been done for example in [2] and [13]. The available benchmarks focus on various aspects of deterministic FSI models and do not include uncertain parameters. Fluid flow problems with an analytical solution of the incompressible

Navier-Stokes equations have been described for example by [4]. Yet, scenarios with an analytical solution of an FSI system have not been published, to the knowledge of the authors. For finding an analytical solution of an FSI problem, the challenge especially is to satisfy the coupling conditions at the fluid-solid interface (4).

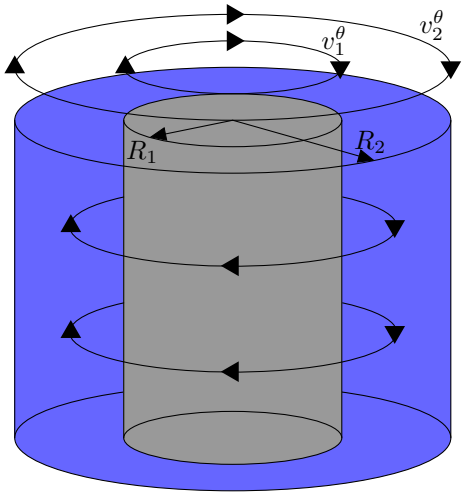

(a) A three-dimensional Taylor-Couette flow system. A fluid is contained in a cylindrical tank with an cylindrical inner wall. Both walls are arranged concentrically and rotate at different speed v_1^θ and v_2^θ. Depending on the boundary velocities, different fluid flow fields emerge.

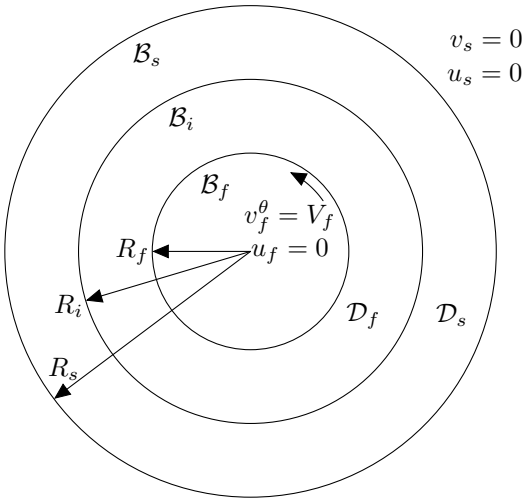

(b) A two-dimensional cut-plane of the Taylor-Couette flow system with an additional solid domain $\mathcal{D}_s$ surrounding the fluid domain $\mathcal{D}_f$. The illustration indicates the geometry and boundary conditions of the benchmark problem.

Figure 1: The Taylor-Couette flow system in three dimensions and with a surrounding solid domain.

In the following, we analytically derive a non-trivial solution of the FSI equations (1) - (4) based on the Taylor-Couette flow system. As shown in fig. 1a, a Taylor-Coutte flow system consists of two concentrically arranged cylinders, which rotate at different angular paces. At moderate to high angular speed, the flow field develops circular revolutions. At lower speed, a laminar velocity field develops. On a cut plane in two dimensions, this velocity field can be described explicitly in polar coordinates. This scenario can be extended to a setup in which another solid domain is located around the fluid domain as shown in fig. 1b. The figure also indicates the Dirichlet boundary conditions of the problem. Velocity and displacement of the solid domain, v_s and u_s, are set to zero at the outer solid boundary $\mathcal{B}_s$, (9), (10). The displacement u_f of the inner fluid boundary $\mathcal{B}_f$ is also set to zero, (13). The fluid boundary velocity in angular direction v_f^θ is of a non-zero value V_f, (11). The radial velocity v_f^r at the boundary is set to zero, (12). To summarise the Dirichlet boundary conditions, we have

$$v_s|_{\mathcal{B}_s} = 0, \tag{9}$$
$$u_s|_{\mathcal{B}_s} = 0, \tag{10}$$
$$v_f^\theta|_{\mathcal{B}_f} = V_f, \tag{11}$$
$$v_f^r|_{\mathcal{B}_f} = 0, \tag{12}$$
$$u_f|_{\mathcal{B}_f} = 0. \tag{13}$$

At the fluid-solid interface $\mathcal{B}_i$ the shear stress of the flow field yields to a displacement force of the solid material in angular direction.

In two dimensions the system of partial differential equations (1) - (4) in Cartesian coordinates can be transformed into a system of ordinary differential equations in polar coordinates. For laminar flow, it can be assumed, that there is no radial velocity or displacement. Additionally, the angular derivative of the

velocity and displacement field can be assumed to be zero. With these two assumptions, the coordinate transformation leads to the following system of stochastic ordinary differential equations on a centerline $[R_f, R_s]$:

$$\rho\nu\left(\partial_{rr}v^\theta(r,\omega)+\frac{1}{r}\partial_r v^\theta(r,\omega)-\frac{1}{r^2}v^\theta(r,\omega)\right)=0,\quad r\in[R_f,R_i],\ \omega\in\Omega, \tag{14}$$

$$\frac{\rho}{r}(v^\theta(r,\omega))^2-\partial_r p(r,\omega)=0,\quad r\in[R_f,R_i],\ \omega\in\Omega, \tag{15}$$

$$\mu(\omega)\left(\partial_{rr}u^\theta(r,\omega)+\frac{1}{r}\partial_r u^\theta(r,\omega)-\frac{1}{r^2}u^\theta(r,\omega)\right)=0,\quad r\in[R_i,R_s],\ \omega\in\Omega, \tag{16}$$

$$\rho\nu\partial_r v^\theta(R_i,\omega)+\mu(\omega)\left(\partial_r u^\theta(R_i,\omega)-\frac{1}{R_i}u^\theta(R_i,\omega)\right)=0,\quad \omega\in\Omega. \tag{17}$$

Next, we decouple the dependency of the state variables v^θ, p and u^θ on the geometric and the stochastic domain. We describe the stochastic part by means of the generalised Polynomial Chaos (PC) expansion [14]. This approach utilises series of orthogonal polynomials in order to represent the dependency of the random variables on the stochastically distributed input parameters. According to the Askey-scheme, Legendre polynomials ψ_k can be used for uniformly distributed input parameters. For $r\in[R_f,R_s]$ and $\omega\in\Omega$ we expand the variables and parameters to

$$\left[v^\theta(r,\omega),p(r,\omega),u^\theta(r,\omega)\right]=\left[\sum_{k=0}^{\infty}v_k^\theta(r)\psi_k(\omega),\sum_{k=0}^{\infty}p_k(r)\psi_k(\omega),\sum_{k=0}^{\infty}u_k^\theta(r)\psi_k(\omega)\right], \tag{18}$$

$$\left[\mu(\omega),V(\omega)\right]=\left[\sum_{k=0}^{\infty}\mu_k\psi_k(\omega),\sum_{k=0}^{\infty}V_k\psi_k(\omega)\right]. \tag{19}$$

The coefficients of the random input parameters can be calculated by the projection

$$\mu_k=\frac{1}{\|\psi_k\|^2_{L^2(\Omega)}}\int_\Omega\mu(\omega)\psi_k(\omega)d\omega,\qquad k=0,\dots. \tag{20}$$

The expansion coefficients of the velocity, pressure and displacement are the variables, the system of stochastic ordinary equations (14) - (17) is to be solved for. We insert (18) and (19) into the system (14) - (17) and apply a Galerkin projection on the stochastic space spanned by the Legendre polynomials. With that, we obtain

$$\rho\nu\left(\partial_{rr}v_k^\theta(r)+\frac{1}{r}\partial_r v_k^\theta(r)-\frac{1}{r^2}v_k^\theta(r)\right)=0,\quad r\in[R_f,R_i], \tag{21}$$

$$\frac{\rho}{r}\sum_{j,l=0}^{\infty}v_j^\theta(r)v_l^\theta(r)c_{jlk}-\partial_r p_k(r)=0,\quad r\in[R_f,R_i], \tag{22}$$

$$\sum_{j,l=0}^{\infty}\mu_j\left(\partial_{rr}u_l^\theta(r)+\frac{1}{r}\partial_r u_l^\theta(r)-\frac{1}{r^2}u_l^\theta(r)\right)c_{jlk}=0,\quad r\in[R_i,R_s], \tag{23}$$

$$\rho\nu\partial_r v_k^\theta(R_i)+\sum_{j,l=0}^{\infty}\mu_j\left(\partial_r u_l^\theta(R_i)-\frac{1}{r}u_l^\theta(R_i)\right)c_{jlk}=0, \tag{24}$$

$$\text{for each PC mode } k=0,\dots.$$

Hereby, the third order stochastic Galerkin tensor is defined by

$$c_{jlk}:=\frac{\langle\psi_j\psi_l,\psi_k\rangle}{\langle\psi_k,\psi_k\rangle},\quad j,l,k=0,\dots. \tag{25}$$

The equations defining the velocity and the displacement field, (21) and (23), respectively, are Euler equations, for which analytical solutions are known [11]. The pressure distribution can be calculated from

the first order differential equation (22). Taking into account the boundary conditions (9) - (13) and the coupling condition (24), one can derive the following analytical solution.

$$v_k^\theta(r) = \frac{V_k R_f}{R_f^2 - R_i^2}\left(r - \frac{R_i^2}{r}\right), \tag{26}$$

$$p_k(r) = \frac{\rho R_f^2}{(R_f^2 - R_i^2)^2}\left(\frac{r^2}{2} + 2R_i^2(ln(R_i) - ln(r)) - \frac{R_i^4}{2r^2}\right)\sum_{j,l=0}^{\infty} V_j V_l c_{jlk}, \tag{27}$$

$$u_k^\theta(r) = a_k r + \frac{b_k}{r}, \tag{28}$$

$$\text{with } a_k = -\frac{b_k}{R_s^2},$$

$$\sum_{j,l=0}^{\infty} \mu_j c_{jlk} b_l = \rho\nu \frac{R_f R_i^2 V_k}{R_f^2 - R_i^2}, \tag{29}$$

$$\text{for } k = 0, \ldots.$$

The PC modes of the angular velocity v_k^θ in the fluid domain and the angular displacement u_k^θ of the solid domain show the same basic dependency on the radius r, see (26) and (28). The coefficients of all three state variables depend on the radii and the uncertain input parameters. The calculation of the coefficients of the displacement field a_k and b_k involves the evaluation of an infinite linear system of equations (29). As only the first two values of μ_k are non-zero, and b_k converges linearly to zero, we can truncate the sum on the left hand side of (29) at a moderate number. Solving the resulting finite system of linear equations directly, approximates the coefficients b_k at a still high accuracy.

4 Numerical Results

We consider the analytically solvable problem from the previous section to verify a numerical solver for FSI problems with uncertain parameters. The solver has been implemented by the authors within the open-source finite element software package HiFlow^3 [1, 12]. The handling of the stochastic space is again based on the generalised PC expansion with Legendre polynomials. By means of a Galerkin projection on the PC space, the solver follows an intrusive approach. For the numerical solver, the PC expansion is truncated at a certain number of modes M:

$$[v(x,\omega), p(x,\omega)] \approx \left[\sum_{k=0}^{M} v_k(x)\psi_k(\omega), \sum_{k=0}^{M} p_k(x)\psi_k(\omega)\right], \qquad x \in \mathcal{D}_f,\ \omega \in \Omega, \tag{30}$$

$$u(x,\omega) \approx \sum_{k=0}^{M} u_k^\theta(x)\psi_k(\omega), \qquad x \in \mathcal{D}_s,\ \omega \in \Omega. \tag{31}$$

We have the following relation between the maximal degree of the Legendre polynomials P, the number of stochastical independent parameters N, and the number of PC modes M [6]:

$$M + 1 = \frac{(N+P)!}{N!P!}. \tag{32}$$

FSI problems naturally have the dualism of the fluid flow equations being formulated in the Eularian perspective (1), (2) and the structure equations being stated in the Lagrangian perspective (3). There are several numerical approaches in matching the two perspectives. With the aim to develop an intrusive solver, it is suitable to use a monolithic approach for the interaction of fluid and structure, as for example the arbitrary Lagrangian-Eularian (ALE) method [5]. However, the ALE-mapping of the fluid domain incorporates further non-linearities in the fluid flow equations. Inserting the PC expansions (30) in these equations leads to the occurrence of higher order stochastic Galerkin tensors. To reduce the complexity, we model the PC modes of the ALE-displacement $u_k^{\mathrm{ALE}}|_{\mathcal{D}_f}$ not as coefficients of the regular PC expansion, but as continuous continuation of the structural displacement PC modes:

$$u_k^{\mathrm{ALE}}|_{\mathcal{B}_i} = u_k|_{\mathcal{B}_i} \tag{33}$$

After inserting the PC expansions (30), (31) and (33) in the ALE version of the FSI equations (1) - (4) and applying the Galerkin projection on the Legendre polynomial basis, the equations read as follows

$$\sum_{j=0}^{M}\sum_{l=0}^{M} J_k F_k^{-1}(\hat{v}_j\cdot\nabla)\hat{v}_l c_{jlk} + \frac{1}{\rho}\nabla\cdot J_k\hat{p}_k F_k^{-T} - J_k\nu\nabla\cdot(\nabla\hat{v}_k F_k^{-1} + F_k^{-T}\nabla\hat{v}_k^T)F_k^{-T} = 0, \quad \text{in } \hat{\mathcal{D}}_f, \tag{34}$$

$$J_k \mathrm{tr}(\nabla\hat{v}_k F_k^{-T}) = 0, \quad \text{in } \hat{\mathcal{D}}_f, \tag{35}$$

$$\alpha\Delta u_k^{\mathrm{ALE}} = 0, \quad \text{in } \hat{\mathcal{D}}_f, \tag{36}$$

$$-\nabla\cdot\left(\sum_{j=0}^{M}\sum_{l=0}^{M}\left(\lambda_j(\nabla\cdot u_l)I c_{jlk} + \mu_j(\nabla u_l + \nabla u_l^T)\right)c_{jlk}\right) = 0, \quad \text{in } \mathcal{D}_s, \tag{37}$$

$$\left(\rho\nu(\nabla\hat{v}_k F_k^{-1} + F_k^{-T}\nabla\hat{v}_k^T) - \hat{p}_k I\right) n_f$$
$$-\left(\sum_{j=0}^{M}\sum_{l=0}^{M}\left(\lambda_j(\nabla\cdot u_l)I + \mu_j(\nabla u_l + \nabla u_l^T)\right)c_{jlk}\right) n_s = 0, \quad \text{on } \mathcal{B}_i, \tag{38}$$

$$k = 0, \ldots, M,$$

where $F_k := \nabla u_k^{\mathrm{ALE}} + I$ and $J_k := \det(F_k)$ denote the deformation gradient tensor and the determinant of the same in the respective PC mode $k = 0, \ldots, M$. The hat sign indicates the definition of the fluid flow variables with respect to the ALE reference domain $\hat{\mathcal{D}}_f$. Equation (36) ensures a smooth transition of the ALE displacement in the fluid flow domain. The diffusion parameter α has to be chosen very small, minimising the diffusive effect on the solid displacement.

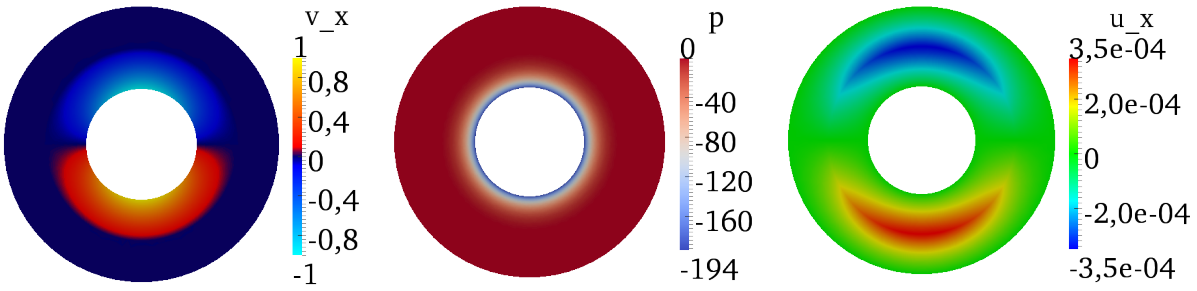

(a) Expected values of the velocity in x-direction, the pressure and the displacement in x-direction (from left to right).

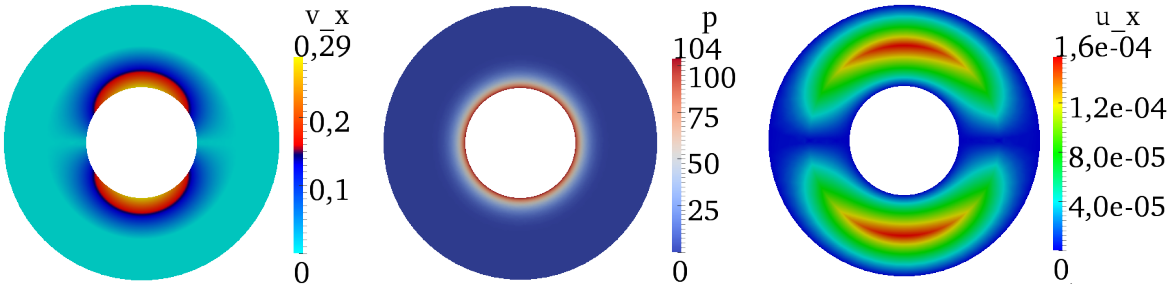

(b) Standard deviation of the velocity in x-direction, the pressure and the displacement in x-direction (from left to right).

Figure 2: Visualization of the simulation results for the presented test problem.

We linearise the non-linear system of equations (34) - (38) with the exact Newton method. Spatial discretisation is achieved by the stable combination of triangular finite elements of second order for the

velocity and the displacement modes and of first order for the pressure modes. The resulting linear system of equations is solved by a GMRES algorithm with incomplete LU-decomposition preconditioning.

Parameter	Symbol	Value
Radii	$R_f,\ R_i,\ R_s$	$0.2,\ 0.35,\ 0.5$
Viscosity, density	$\nu,\ \rho$	$1 \times 10^3,\ 1.5 \times 10^{-3}$
Boundary velocity	$V_0,\ V_1$	$1,\ 0.5$
Reynolds number	Re	50 - 150
Young's modulus	$Y_0,\ Y_1$	$5.6,\ 2.8 \times 10^3$
Poisson's ratio	γ	0.4

Table 1: List of parameters for the numerical simulation benchmark.

Fig. 2 shows the computed expected value and the standard deviation of several variables. The parameters, which have been used for the test scenario in this paper are summarised in table 1. In the fluid domain, the expected flow and pressure field develops as prescribed by the Taylor-Couette flow equations. The angular displacement is highest at the fluid-structure interface and smoothly decreases towards the inner and the outer boundary.

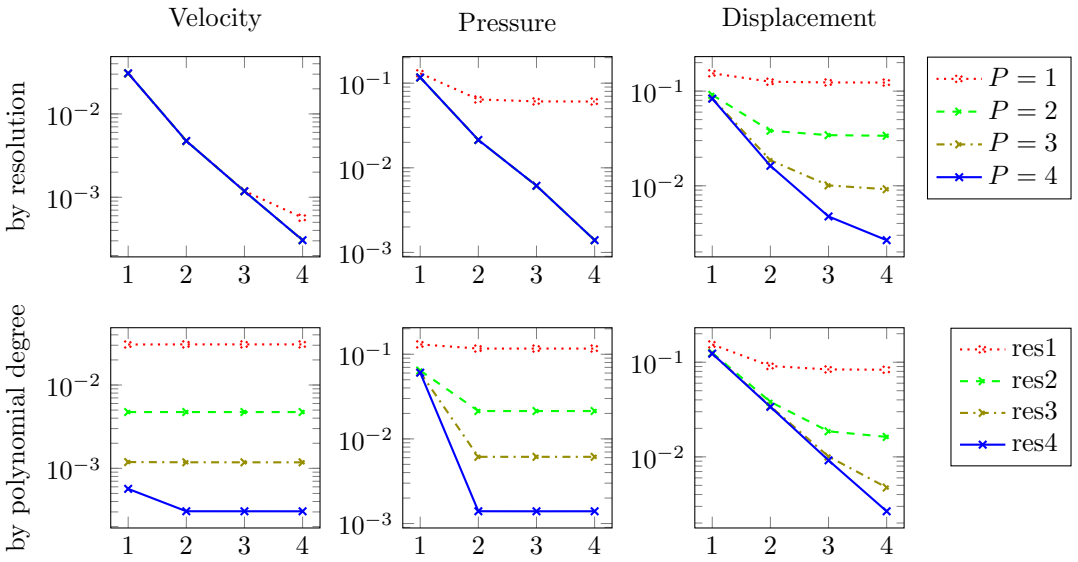

Figure 3: Numerical convergence results with respect to the L^2-error (39). The upper row shows the error with respect to the resolution of the discrete geometric domain. For each resolution level, the mesh size is halved. The lower row shows the error with respect to the maximal polynomial degree of the stochastical polynomial basis.

We compute the error with respect to the analytical solution by the relative L^2-error:

$$e_{L^2} := \frac{\|U_h - U\|_{L^2(\mathcal{D},\Omega)}}{\|U\|_{L^2(\mathcal{D},\Omega)}}, \tag{39}$$

$$\|U\|^2_{L^2(\mathcal{D},\Omega)} := \int_\Omega \int_\mathcal{D} |U(x,\omega)|^2 \mathrm{d}x\rho(\omega)\mathrm{d}\omega, \tag{40}$$

where U can be any of the state variables. Fig. 3 shows the relative L^2-error convergence of the computed results with respect to the spatial domain resolution and with respect to the maximal polynomial degree P of the PC expansion. With the choice of the parameters, the expected value and the first PC mode

referring to the velocity field are non-zero. The other velocity PC-modes are zero. Hence, for $P > 1$, the velocity error does note depend on the maximal polynomial degree of the PC expansion. The results for the velocity are in accordance with the independence on the PC expansion truncation. The pressure has one additional non-zero PC mode. For $P = 1$, this mode is not considered, but for $P \geq 2$, it is taken into account. Accordingly, we observe an accuracy gain for the pressure from $P = 1$ to $P = 2$. The PC modes of the displacement are zero if the mode index refers to a polynomial degree of the velocity parameter expansion of higher than one. This leads to a linear convergence of the displacement error with respect to the polynomial degree. With regard to the spatial discretisation, the geometry has to be resolved fine enough in order to observe convergence with respect to the PC expansion. Vice versa, the PC expansion has to be accurate enough to observe a quadratic convergence with respect to mesh refinement.

5 Conclusion and Outlook

In this work, we presented a test problem for FSI simulations with uncertain input parameters. The test problem is based on the Taylor-Couette flow with an additional solid domain surrounding the fluid domain. We derived an analytical solution of the two-dimensional case in polar coordinates. For the Uncertainty Quantification we utilised a Polynomial Chaos expansion. The test problem can be used for benchmarking numerical FSI solvers relying on Cartesian coordinates. The intrusive UQ solver for FSI problems implemented by the authors shows well accordance with the theory with respect to the numerical convergence.

Future work will include the application of the verified solver to more complex three-dimensional FSI problems with uncertain parameters. One of these applications is given by aortic blood flow with an elastic vessel wall. Hereby, the imprecisely known stiffness of the vessel wall can be modelled as uncertain input parameter. Measurement inaccuracies are also given with respect to the blood flow velocity field and the pressure ratios. The propagation of inaccuracies can be described by simulations which include the quantification of uncertainties.

For the scalability of the solver to a higher complexity in the considered problems, specific linear solving routines can be developed. The discrete system of equations has a block structure, both with respect to the fluid-structure components and with respect to the intrusive Uncertainty Quantification approach. This structure can be exploited for the derivation of efficient preconditioners.

6 Acknowledgement

This work was performed on the computational resource bwForCluster MLS&WISO (Production) and the authors acknowledge this support by the state of Baden-Württemberg through bwHPC and the German Research Foundation (DFG) through grant INST 35/1134-1 FUGG. The authors acknowledge support from the Heidelberg Institute for Theoretical Studies (HITS).

References

[1] H. Anzt, W. Augustin, M. Baumann, T. Gengenbach, T. Hahn, A. Helfrich-Schkarbanenko, V. Heuveline, E. Ketelaer, D. Lukarski, A. Nestler, S. Ritterbusch, S. Ronnas, M. Schick, M. Schmidtobreick, C. Subramanian, J.-P. Weiss, F. Wilhelm, and M. Wlotzka. *HiFlow^3: A Hardware-Aware Parallel Finite Element Package*, pages 139–151. Springer Berlin Heidelberg, Berlin, Heidelberg, 2012.

[2] Klaus-Jürgen Bathe and Gustavo A Ledezma. Benchmark problems for incompressible fluid flows with structural interactions. *Computers & structures*, 85(11):628–644, 2007.

[3] Bongjae Chung and Juan Raul Cebral. Cfd for evaluation and treatment planning of aneurysms: Review of proposed clinical uses and their challenges. *Annals of Biomedical Engineering*, 43(1):122–138, 2015.

[4] C. Ross Ethier and D. A. Steinman. Exact fully 3d navier–stokes solutions for benchmarking. *International Journal for Numerical Methods in Fluids*, 19(5):369–375, 1994.

[5] Luca Formaggia, Alfio Quarteroni, and Alessandro Veneziani. *Cardiovascular Mathematics: Modeling and simulation of the circulatory system*, volume 1. Springer Science & Business Media, 2010.

[6] Roger G Ghanem and Pol D Spanos. *Stochastic finite elements: a spectral approach*. Courier Corporation, 2003.

[7] Gerhard A Holzapfel and Ray W Ogden. *Biomechanics of soft tissue in cardiovascular systems*, volume 441. Springer, 2014.

[8] Jonas Kratzke, Nicolai Schoch, Christian Weis, Matthias Müller-Eschner, Stefanie Speidel, Mina Farag, Carsten J. Beller, and Vincent Heuveline. Enhancing 4d pc-mri in an aortic phantom considering numerical simulations, 2015.

[9] Olivier Le Maître and Omar M Knio. *Spectral methods for uncertainty quantification: with applications to computational fluid dynamics*. Springer Science & Business Media, 2010.

[10] Wilmer Nichols, Michael O'Rourke, and Charalambos Vlachopoulos. *McDonald's blood flow in arteries: theoretical, experimental and clinical principles*. CRC Press, 2011.

[11] Andrei D Polyanin and Valentin F Zaitsev. Exact solutions for ordinary differential equations. *Campman and Hall/CRC*, 2, 1995.

[12] M. Schick, V. Heuveline, and O. P. Le Maître. A newton–galerkin method for fluid flow exhibiting uncertain periodic dynamics. *SIAM/ASA Journal on Uncertainty Quantification*, 2(1):153–173, 2014.

[13] Stefan Turek, Jaroslav Hron, Mudassar Razzaq, Hilmar Wobker, and Michael Schäfer. Numerical benchmarking of fluid-structure interaction: A comparison of different discretization and solution approaches. In *Fluid Structure Interaction II*, pages 413–424. Springer, 2011.

[14] Dongbin Xiu and George Em Karniadakis. The wiener–askey polynomial chaos for stochastic differential equations. *SIAM journal on scientific computing*, 24(2):619–644, 2002.

Preprint Series of the Engineering Mathematics and Computing Lab

recent issues

No. 2016-01 Philipp Gerstner, Michael Schick, Vincent Heuveline, Nico Meyer-Hübner, Michael Suriyah, Thomas Leibfried, Viktor Slednev, Wolf Fichtner, Valentin Bertsch: A Domain Decomposition Approach for Solving Dynamic Optimal Power Flow Problems in Parallel with Application to the German Transmission Grid

No. 2015-04 Philipp Gerstner, Vincent Heuveline, Michael Schick : A Multilevel Domain Decomposition approach for solving time constrained Optimal Power Flow problems

No. 2015-03 Martin Wlotzka, Vincent Heuveline: Block-asynchronous and Jacobi smoothers for a multigrid solver on GPU-accelerated HPC clusters

No. 2015-02 Nicolai Schoch, Fabian Kißler, Markus Stoll, Sandy Engelhardt, Raffaele de Simone, Ivo Wolf, Rolf Bendl, Vincent Heuveline: Comprehensive Pre- & Post-Processing for Numerical Simulations in Cardiac Surgery Assistance

No. 2015-01 Teresa Beck, Martin Baumann, Leonhard Scheck, Vincent Heuveline, Sarah Jones: Comparison of mesh-adaptation criteria for an idealized tropical cyclone problem

No. 2014-02 Christoph Paulus, Stefan Suwelack, Nicolai Schoch, Stefanie Speidel, Rüdiger Dillmann, Vincent Heuveline: Simulation of Complex Cuts in Soft Tissue with the Extended Finite Element Method (X-FEM)

No. 2014-01 Martin Wlotzka, Vincent Heuveline: A parallel solution scheme for multiphysics evolution problems using OpenPALM

No. 2013-04 Nicolai Schoch, Stefan Suwelack, Stefanie Speidel, Rüediger Dillmann, Vincent Heuveline: Simulation of Surgical Cutting in Soft Tissue using the Extended Finite Element Method (X-FEM)

No. 2013-03 Martin Wlotzka, Edwin Haas, Philipp Kraft, Vincent Heuveline, Steffen Klatt, David Kraus, Klaus Butterbach-Bahl, Lutz Breuer: Dynamic Simulation of Land Management Effects on Soil N2O Emissions using a coupled Hydrology-Ecosystem Model

No. 2013-02 Martin Baumann, Jochen Förstner, Bernhard Vogel, Vincent Heuveline, Jonas Kratzke, Sebastian Ritterbusch, Heike Vogel: Model-based Visualization of Instationary Geo-Data with Application to Volcano Ash Data

No. 2013-01 Martin Schindewolf, Björn Rocker, Wolfgang Karl, Vincent Heuveline: Evaluation of two Formulations of the Conjugate Gradients Method with Transactional Memory

No. 2012-07 Andreas Helfrich-Schkarbanenko, Vincent Heuveline, Roman Reiner, Sebastian Ritterbusch: Bandwidth-Efficient Parallel Visualization for Mobile Devices

No. 2012-06 Thomas Henn, Vincent Heuveline, Mathias J. Krause, Sebastian Ritterbusch: Aortic Coarctation simulation based on the Lattice Boltzmann method: benchmark results

No. 2012-05 Vincent Heuveline, Eva Ketelaer, Staffan Ronnas, Mareike Schmidtobreick, Martin Wlotzka: Scalability Study of HiFlow^3 based on a Fluid Flow Channel Benchmark

Preprint Series of the Engineering Mathematics and Computing Lab (EMCL)

http://emcl.iwr.uni-heidelberg.de